



ELSEVIER
MASSON



Disponible en ligne sur
SciVerse ScienceDirect
www.sciencedirect.com

Elsevier Masson France
EM|consulte
www.em-consulte.com

IRBM

IRBM 34 (2013) 349–356

Research in Imaging and Health Technologies

3D articulated growth model of the fetus skeleton, envelope and soft tissues

A. Serrurier^a, S. Dahdouh^{a,*}, G. Captier^c, V. Calmels^b, C. Adamsbaum^{a,b,d}, I. Bloch^a

^a Institut Mines-Telecom, Telecom ParisTech/CNRS LTCI/Whist Lab, 46, rue Barrault, 75013 Paris, France

^b General and Pediatric Radiology Departments, Bicêtre Hospital, AP-HP, Paris, France

^c Anatomy laboratory, Montpellier-1 University, Montpellier, France

^d Paris-Sud University, 91405 Orsay cedex, France

Received 13 May 2013; received in revised form 3 June 2013; accepted 28 June 2013

Available online 23 September 2013

Abstract

Fetal dosimetry studies require the development of accurate 3D models of the fetus. This paper proposes a 3D articulated fetal growth model including skeleton, body envelope, brain and lungs based on medical images of ten different fetuses acquired in clinical routine. The structures of interest were semi-manually segmented from the images and surface meshes were generated. A generic mesh of each structure has been deformed towards the segmented ones. By interpolating linearly between the subjects of the database, each structure can be estimated at any age and in any position. This process results in an automated model, the operator being only required to specify the age and position of the desired estimated fetus. © 2013 Elsevier Masson SAS. All rights reserved.

1. Introduction

In order to assess the impact of radiofrequency waves on human beings, dosimetry studies have to be performed. To do so, reliable human models have to be constructed. While many adult models have been developed, only few studies have focused on embryo [1] and fetus [2]. To our knowledge, no *in silico* model of fetus growth has been proposed in the literature. Our objective in this paper is thus to develop a three-dimensional (3D) growth model of the fetus including fetal skeleton, body envelope, brain and lungs. It aims at estimating fetuses at any age and position from 14 to 32 weeks of amenorrhea (WA). Beyond the scope of dosimetry, such a model will also be useful in fields like developmental studies, medical research, teaching or surgery simulations. The construction of the model and a few selected results are presented in this paper.

2. Material and methods

2.1. Data

Several sets of medical images of various modalities representing different fetuses were used for this project, as

summarized in Table 1. Using complementary 3D imaging modalities allows us to cover a large range of ages and visible structures. All the images were recorded on pregnant women during medical examinations except two sets of micro-Computer Tomography (μ CT) recorded on fetuses conserved in formalin for several decades.

2.2. Algorithm

In order to construct a 3D articulated growth model from these data, a multi-steps algorithm has been developed as shown in Fig. 1. First, a semi-manual strategy is applied in order to obtain reliable 3D meshes from medical imaging data. These meshes are then used to construct a growth evolution model of the fetal body throughout pregnancy. The whole method is detailed in the following sections.

2.2.1. Image-based 3D meshes construction

Different image processing strategies have been used in order to retrieve the structures of interest according to data type. For Magnetic Resonance Imaging (MRI) data, brain and lungs have been segmented using the method presented in Anquez et al. [3], while in 3D Ultrasound (US) segmentation has been performed manually due to the very low signal to noise ratio. Semi-automatic segmentation procedures have been used for the skeleton and envelope segmentation on CT-scan and

* Corresponding author.

E-mail address: dahdouh@telecom-paristech.fr (S. Dahdouh).

Table 1
Data characteristics.

Modality	Pregnancy stage(WA)	Slice thickness(mm)	Image resolution(mm/px)	Subject	Structures of interest
CT	27	1.2	0.64	In vivo	Skeleton
CT	32	1	0.96	In vivo	Skeleton + envelope
μ CT	14	0.048	0.036	Formalin	Skeleton + lungs + brain
μ CT	16	0.144	0.036	Formalin	Skeleton
MRI	20	0.74	0.74	In vivo	Brain
MRI	26	1.6	1.36	In vivo	Brain + lungs
MRI	30	4	0.94	In vivo	Brain + lungs
MRI	32	4	0.94	In vivo	Brain + lungs
MRI	34.5	4	0.94	In vivo	Brain + lungs
3D US	13	7.6	0.76	In vivo	Brain + lungs

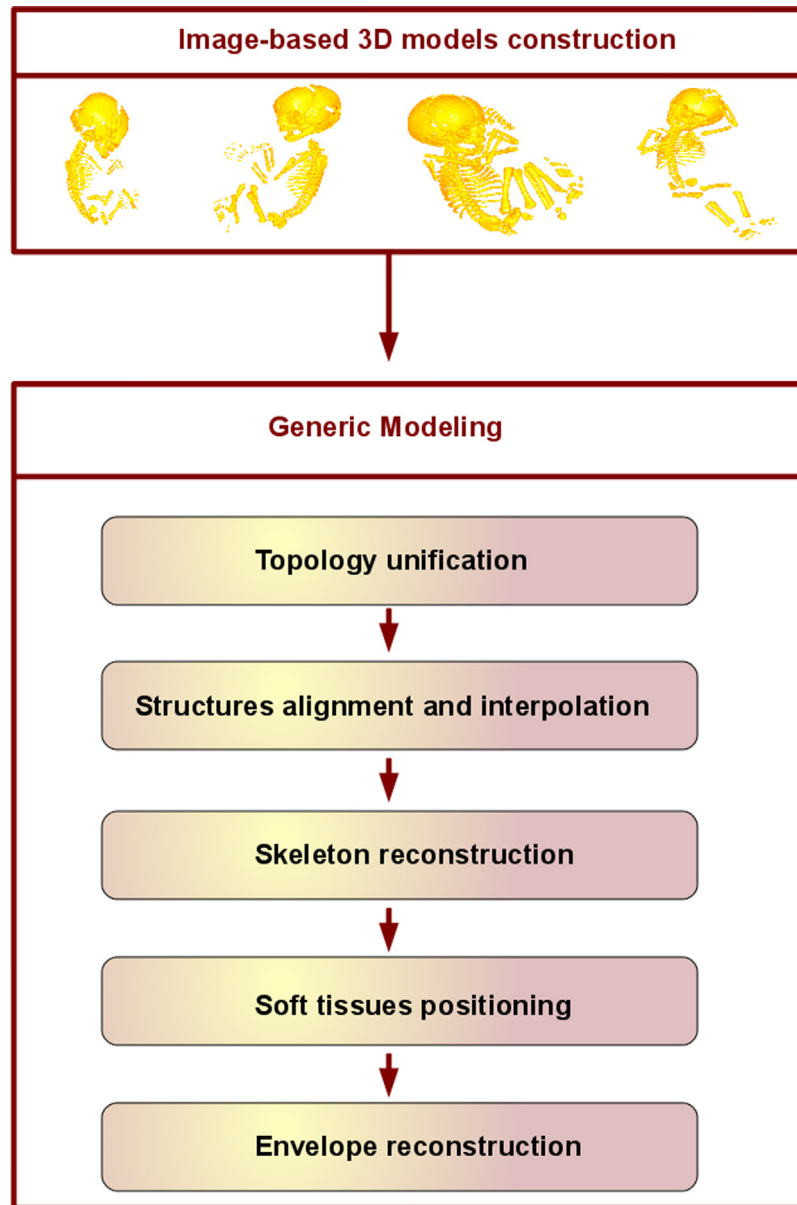


Fig. 1. Global algorithm.

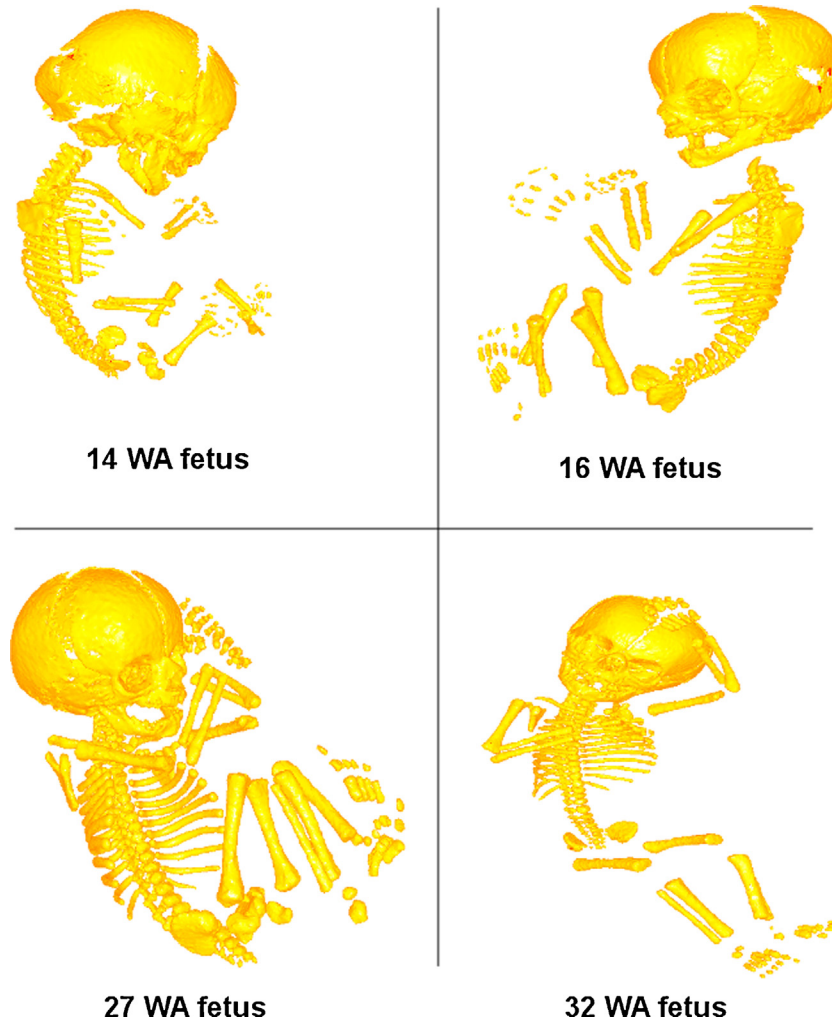


Fig. 2. Semi-manually segmented skeletons from the database.

μ -CT data on which a pre-processing step aiming at enhancing structures contrast and reducing high frequency noise has been applied. A surface triangular mesh has been generated for each structure.

Examples of these semi-manual segmentations can be seen in Fig. 2 where four fetal skeletons at different ages have been segmented.

This process resulted in a database of meshed structures defined as follows: the brain, referring to the addition of the brain and the cerebrospinal fluid, the lungs, viewed as a unique structure composed of two separated parts, and the skeleton, split into 14 substructures within which no relative displacement between the bones is allowed in our model, more specifically:

- the head;
- the trunk and the pelvis together, including the pelvis bones, the spine, the ribs, the clavicles and the scapulas;
- each of the two humerus;
- each of the two forearms;
- each of the two hands;

- each of the two femurs;
- each of the two legs;
- each of the two feet.

2.2.2. Generic modeling

2.2.2.1. Topology unification. In order to be able to perform an interpolation between the different meshes of the database, one needs a similar topology for the meshes of equivalent structures at each age. Thus, a generic mesh has been chosen as reference for each structure. The meshes derived from the CT data at 32 WA for the skeleton sections, being more precise and of higher quality than the others, have been chosen. For similar reasons, brain and lungs from the MRI images at 34.5 WA were used. For each structure, the chosen generic mesh has been deformed towards the equivalent mesh at each age using a set of manually and automatically selected landmarks on both meshes. For soft tissues, a deformation based on a 3D deformation method based on the 3D Moving Least Square (MLS) [4] has been performed whereas for some of the skeleton structures, this operation has been preceded by a 3D Kriging [5] one using the same landmarks.

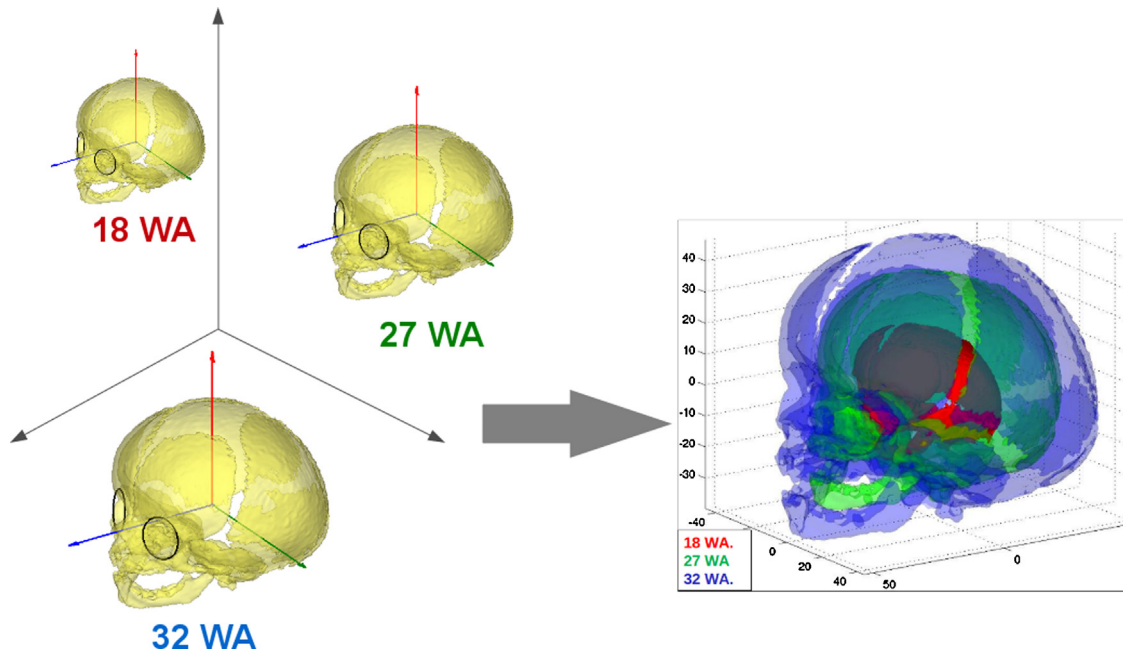


Fig. 3. Fetus skulls at different ages with their local coordinate system and superposition of these skulls in the same local coordinate system.

The deformed meshes have finally been substituted to the original ones for the rest of the study, providing for each structure a mesh of same topology at all ages.

2.2.2.2. Structures alignment and interpolation. In order to align the structure meshes at different ages, a local coordinate system has been defined for each of the skeleton sections and each of the soft tissues based on anatomic and geometric considerations.

An example is shown in Fig. 3, where anatomic characteristics such as ocular globes are used to define a local coordinate system which allows the superposition of the same structure at all ages.

By placing each structure mesh in its local coordinate system, an estimation of the structure shapes at any age using a linear interpolation between the vertices of the meshes is made possible. Since, except for the 14 WA fetus, key ages (e.g the ones where real data are available) for skeleton and soft tissues

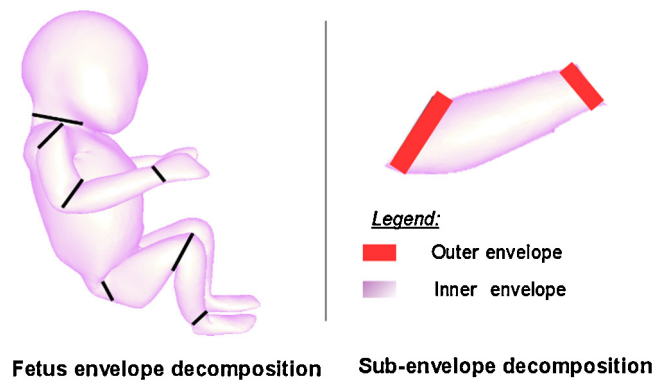


Fig. 4. Envelope decompositions.

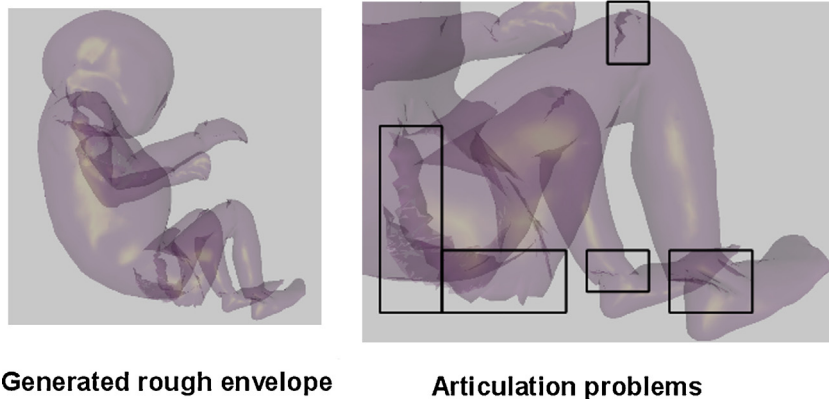


Fig. 5. Rough envelope obtained after Algorithm 2 and zoom on remaining articulation problems.

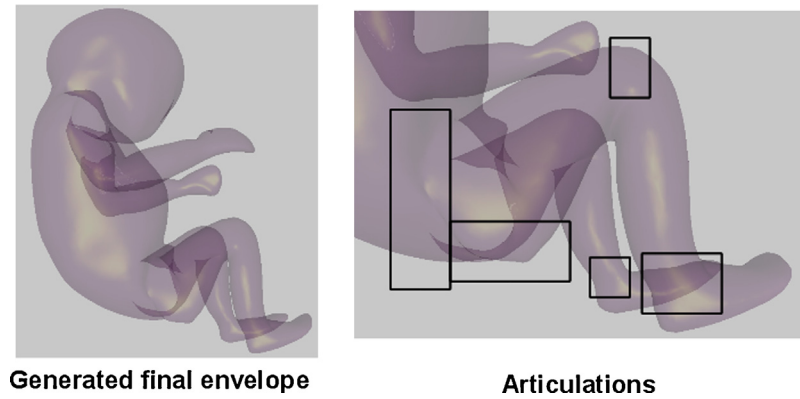


Fig. 6. Resulting envelope obtained after Algorithm 3.

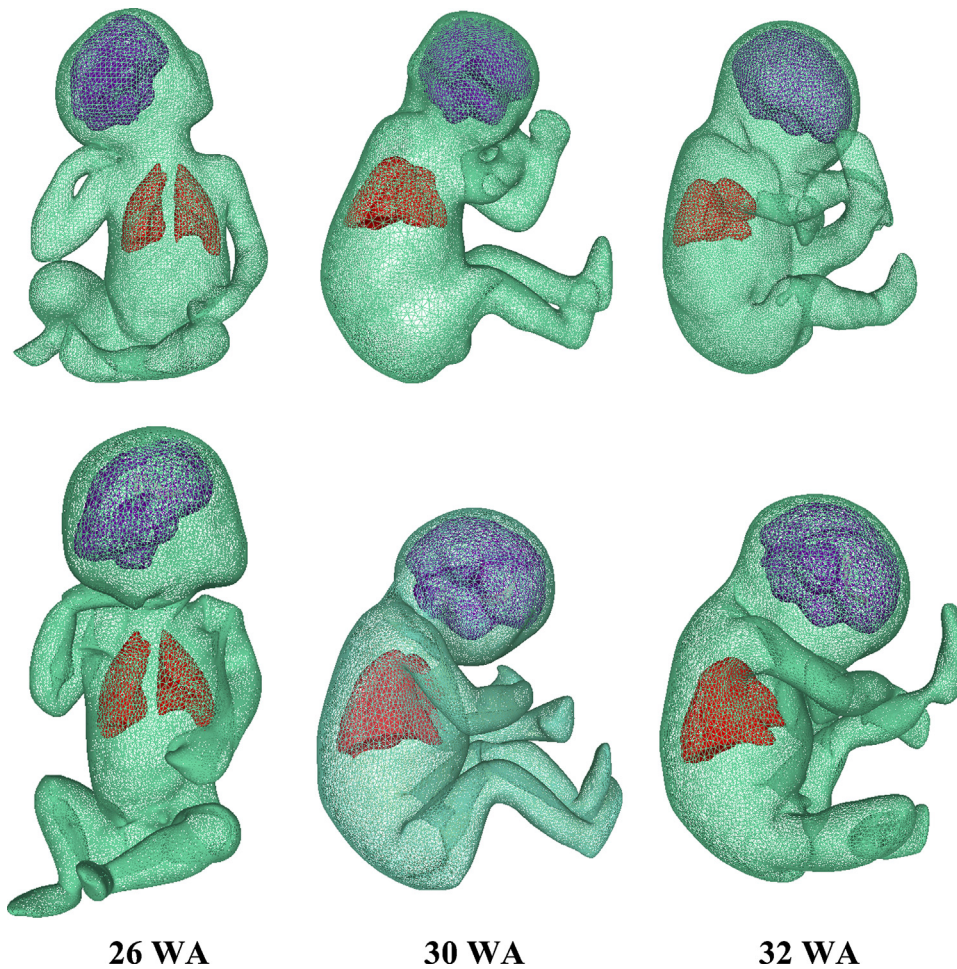


Fig. 7. Three 3D meshes of reference segmented fetuses (top) and their simulated counterparts with our model (bottom).

are not the same, the Algorithm 1 has been applied prior to the interpolation step.

2.2.2.3. Skeleton reconstruction. The various estimated skeleton section meshes are then assembled together to form a fetus in the desired position, the articulations between the skeleton sections being derived from the observed articulations of the fetuses of the database using geometrical considerations.

2.2.2.4. Soft tissues positioning. The estimated soft tissues meshes are finally positioned in relation to their underlying skeleton structures, i.e. the head for the brain, and the spine and rib cage for the lungs, the insertion conflicts being avoided thanks to Algorithm 1.

Algorithm 1 (*Meshes reshaping*).

Data: Soft tissues, Skeleton, *Soft_tissues_key_ages*, *Skeleton_key_ages*

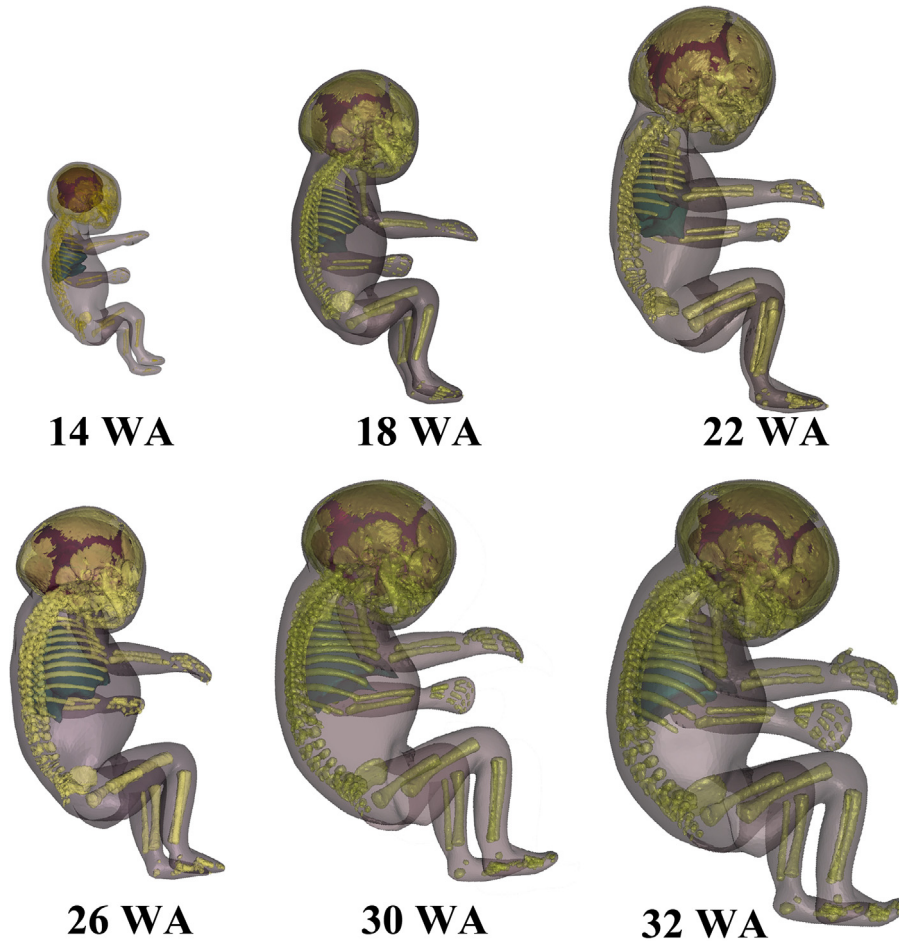


Fig. 8. 3D meshes of fetuses with the same position at different ages.

Result: Soft tissues, Skeleton
foreach Age **do**
if Age \in *Soft_tissues_key_ages* **then**
 Rescale skeleton structure according to soft tissue
end
if Age \in *Skeleton_key_ages* **then**
 Rescale soft tissue according to skeleton
end
end

2.2.2.5. Envelope reconstruction. Since the fetal envelope varies according to the age of the fetus but also, unlike the above structures, according to the desired position of the fetus regardless of its age, a different strategy has to be developed. We decided therefore to use a single generic envelope mesh (the one corresponding to the 32 WA fetus) deformed towards the desired fetus according to the underlying skeleton.

The generic envelope Env is first split into 14 sub-envelopes $Env(i)$ corresponding to the skeletal structures $Sk(i)_{i \in \{1..14\}}$ described in the previous sections. Each sub-envelope is then split into two parts: the inner envelope $in_Env(i)$ corresponding to the middle part of the sub-envelope, and the outer envelope

$out_Env(i)$ corresponding to the parts used as junctions with the other limbs, as shown in Fig. 4.

The generic envelope Env is then deformed using a two step algorithm. The first step ensures the production of a first rough approximation of the envelope, as explained in Algorithm 2.

Algorithm 2 (First step).

Data: $m_Sk(i)_{i \in \{1..14\}}$: $Sk(i)$ of the generic skeleton,
 $d_Sk(i)_{i \in \{1..14\}}$: $Sk(i)$ of the target skeleton, $Env(i)$

Result: $r_in_Env(i)$, $r_out_Env(i)$, $i_in_{\{1..14\}}$

foreach $Sk(i)_{i \in \{1..14\}}$ **do**

$m_points \leftarrow$ Select 500 random vertices on $m_Sk(i)$

$d_points \leftarrow$ Get equivalent vertices on $d_Sk(i)$

$res_Env(i) \leftarrow$ Deform $Env(i)$ using m_points and d_points in a MLS procedure using the Euclidean distance and a mild rigidity factor

$res_Env(i) = r_in_Env(i) \cup r_out_Env(i)$

end

As we can see in Fig. 5, the method's result gives a global idea of the final envelope but in some cases, body articulations are shrunk and twisted whereas in other cases they seem to be separated from the rest of the body.

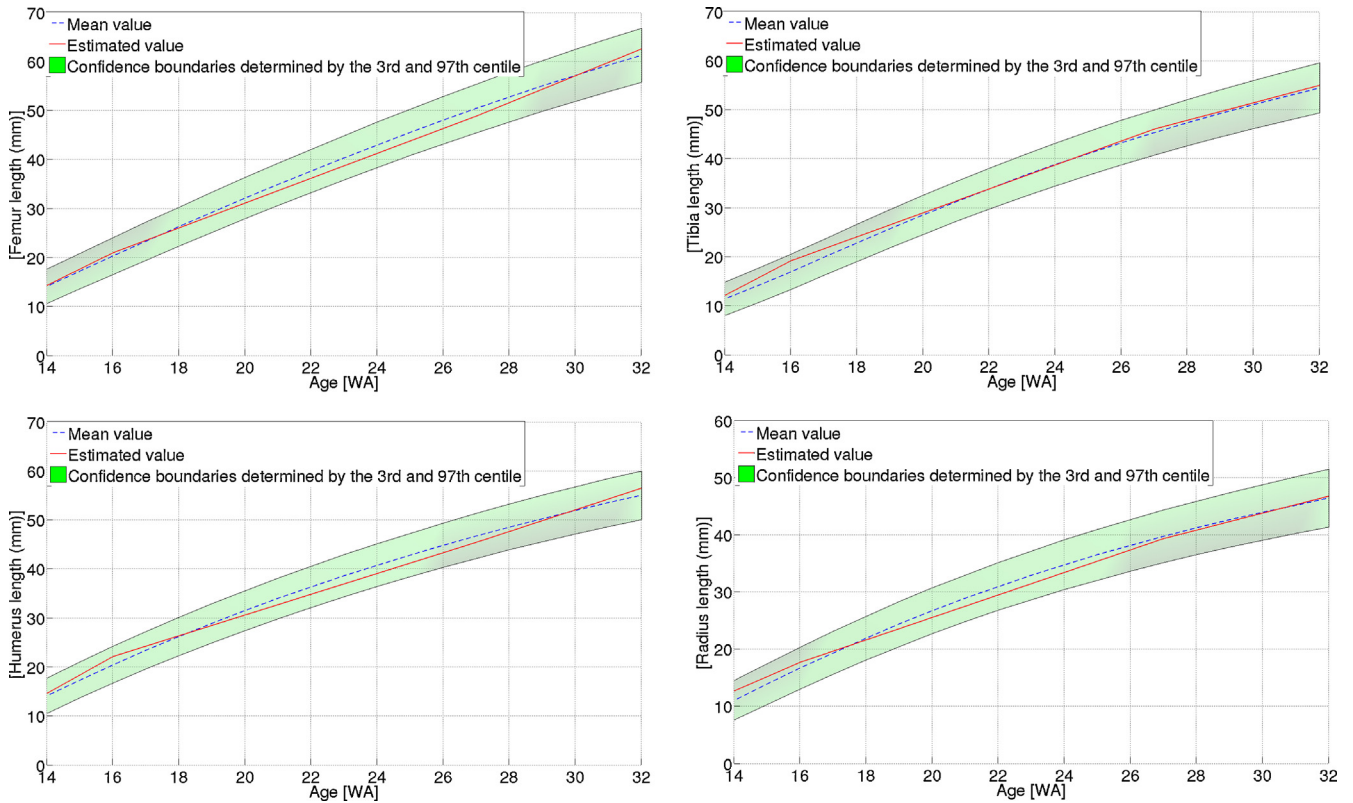


Fig. 9. Means of left and right values for the length of different fetus limbs (femur, tibia, humerus, radius) in relation to fetus ages (red) superimposed on charts values. In each case, the mean chart value as well as the confidence interval defined by the 3rd and 97th centile are also drawn.

In order to address these issues, the outcome of Algorithm 2 is used as a guideline to perform a second deformation of *Env*, handling specifically the articulation problems. The idea consists in constraining strongly the inner envelopes vertices to fit the outcome of Algorithm 2 while relaxing the outer envelope vertices to ensure smooth articulations, as detailed in Algorithm 3. As we can see in Fig. 6, body articulations are now correctly represented and the result seems visually coherent.

Algorithm 3 (Second step).

Data: *in_Env(i)*, *r_in_Env(i)*, *Env*

Result: *res_Env*

foreach *in_Env(i)* **do**

m_points ← Select 2000 random vertices on *in_Env(i)*

d_points ← Get equivalent vertices on *r_in_Env(i)*

res_Env ← Deform *Env* using *m_points* and *d_points* in a MLS procedure using a topological distance and a strong rigidity factor.

end

3. Results

In order to assess the validity of our model, some qualitative and quantitative experiments have been performed.

3.1. Qualitative validation

Two experiments have been carried out to evaluate the model’s behavior with respect to age and position criteria.

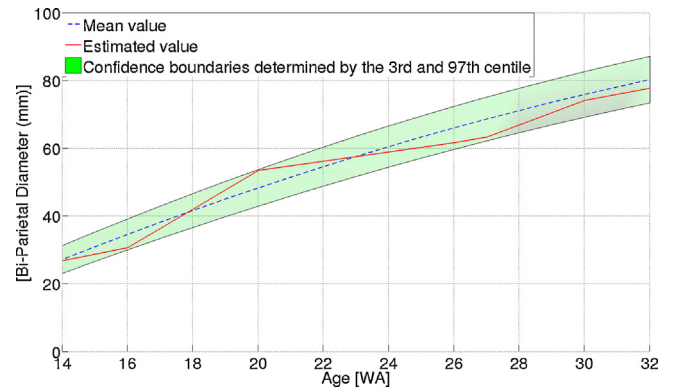


Fig. 10. Bi-parietal diameter of our model in relation to fetus age (red) superimposed on charts values.

First, fetuses at three different ages have been generated and positioned in the same position as reference fetuses taken from the FEMONUM database,¹ as illustrated in Fig. 7. Because the inter-subject variability is not modeled, an exact registration is impossible. Thus, the estimated and reference fetuses have been compared in terms of global shape appearance and soft tissues positioning. Our model seems able to reproduce a real fetus position with its global dimensions and soft tissue positioning preserved. However, since our model articulations do not have

¹ <http://femonum.telecom-paristech.fr/>.

all the freedom degrees that exist in real ones, some positions (like the 26 WA one) could not be reached exactly.

In a second experiment, fetuses with the same position but at different ages have been generated, as illustrated in Fig. 8. Since no mobility degree has been allowed for the spine, it reflects the shape of the fetuses present in the database and the positions at 14 and 32 WA are slightly different, the one at 32 weeks being more curled up. Despite this limitation, the global position is preserved, the soft tissues are well positioned, and the fetal proportions are respected.

3.2. Quantitative validation

In order to assess the validity of the modeled skeletons, some fetal biometry markers have been computed and compared to the literature [6] and to the charts from the French college of fetal ultrasound imaging [7]. The results are given in Fig. 9. As we can see, the values representing the modeled fetus are of the same order as the mean value and are always inside the confidence interval, which seems to validate the proposed approach for skeletal evolution regarding to limbs.

The same comparison is made for the bi-parietal diameter, commonly used in pregnancy follow-up as shown in Fig. 10. As we can see here, the computed values are still within the confidence interval. However, in some cases, the values are closer to the extremities of the interval than to the mean curve. These cases correspond to the ages where information was given either for the soft-tissues or for the skeleton. At these key ages, the model reflects exactly the data and thus the fact that our model does not take into account intra-ages variability.

4. Discussion and conclusion

In this paper, a growth model allowing the construction of a fetus at any age between 14 and 32 WA and placed in any position

has been presented. This process ensures a realistic model but raises also a few limitations due to the heavy processing involved with medical images. The model relies indeed on a limited number of subjects not allowing us to take into account the variability between fetuses of a same age. This induces a bias in the evolution model since inter-individual variability cannot be stretched apart from inter-ages variability. The behavior of the model regarding age and position has been studied and comparisons have been performed with classical charts values. Despite the modest size of the initial database, these two validations have shown that the modeled fetuses fit in terms of biometry measures and visual appearance to real ones. Increasing the size of the image database will naturally improve this fitting and allow even more realistic models. The presented modeling should be used in a near future for dosimetry studies on the fetus.

References

- [1] Smith BR. Visualizing human embryos. *Sci Am* 1999;280:76–81.
- [2] Bibin L, Anquez J, de la Plata Alcalde JP, Boubekeur T, Angelini E, Bloch I. Whole body pregnant woman modeling by digital geometry processing with detailed utero-fetal unit based on medical images. *IEEE Trans Biomed Eng* 2010;57(10):2346–58.
- [3] Anquez J, Bibin L, Angelini E, Bloch I. Segmentation of the fetal envelope on ante-natal MRI. *Int Symp Biomed Imaging* 2010: 896–9.
- [4] Zhu Y, Gortler SJ. 3D Deformation Using Moving Least Squares. *Harvard University Technical Report*; 2007.
- [5] Trochu F. A contouring program based on Dual Kriging interpolation. *Eng Comput* 1993;9:160–77.
- [6] Chittya LS, Altman DG. Charts of fetal size: limb bones. *BJOG* 2002;109:919–29.
- [7] Moeglin D, Talmant C, Duyme M, Lopez AC. Fetal lung volumetry using two- and three-dimensional ultrasound. *Ultrasound Obstet Gynecol* 2005;25:119–27.